ARTICLE

Uploading and Temperature-Controlled Release of Polymeric Colloids via Hydrophilic Emulsion-Templated Porous Polymers

Neil C. Grant, Andrew I. Cooper, and Haifei Zhang*

Department of Chemistry, University of Liverpool, Crown Street, Liverpool L69 7ZD, United Kingdom

ABSTRACT Porous cross-linked poly(*N*-isopropylacrylamide) (PNIPAM) was prepared using high internal phase emulsions as templates. The materials could absorb a large volume of water and swell largely at room temperature. When the aqueous phase was heated above the lower critical solution temperature (LCST) of PNIPAM, the swollen structure could contract and squeeze some of the absorbed liquids out. This capability was utilized in the uploading at room temperature and then release of polystyrene colloids by increasing the temperature above the LCST. The thermoresponsive porous PNIPAM acted like a pump to load and then release the polymer colloids. The multicycles of loading and release were demonstrated to show its efficiency. Importantly, it showed that most of the PS colloids from the second upload onward could be released during the heating cycle.

KEYWORDS: temperature sensitive • polyHIPE • emulsion-templating • controlled release • polymer colloids

INTRODUCTION

Porous materials have a wide range of applications. Among those, porous polymers can be used as scaffolds for tissue engineering and controlled drug release (1, 2). The controlled release from a porous carrier can be realized using one trigger or combined triggers. The trigger sensitivity is a very important parameter for a controlled release process. For porous polymers applied in an aqueous environment, higher porosity and interconnected pores can allow sufficient contact between water and polymer and the free flow of aqueous phase into and out of the structures. As a result of large amount of water being absorbed, the polymer is soft and the network is flexible. This may render the porous polymer a higher sensitivity toward a trigger which is directly affected by transport in water. A highly interconnected porous structure can be prepared using a high internal phase emulsion (HIPE, with an internal phase volume greater than 74.04 v/v %) as template (3, 4). The continuous phase of a HIPE is polymerized and a porous material with a high pore volume can be produced after the removal of the internal phase in the original emulsion. This type of porous materials is known as PolyHIPEs (3). There are many potential applications for polyHIPEs including gas storage (5), as scaffolds for tissue engineering (6), as support for organic synthesis (7), electrochemical sensing (8), and many other applications (4, 9). A variety of polyHIPE and polyHIPE-based materials have been synthesized including hydrophobic polymers (9−11), hydrophilic polymers (12, 13), interpenetrating polymer networks (14), biodegradable polymers (15, 16), and organic−inorganic composites (17, 18). Instead of using conventional surfactants, Pickering HIPEs were also employed to produce polyHIPEs with the use of silica particles (19), titania nanoparticles (20), and polymer particles (21) as stabilizers. Different monomers could be used to produce polyHIPEs with different functionalities (3, 4). The surface properties of formed polyHIPEs could also be modified with plasma treatment (22) or functionalized by click chemistry (23).

Poly(*N*-isopropylacrylamide) (PNIPAM) has been the most widely used temperature responsive polymer (24). PNIPAM exhibits a sharp phase transition with the low critical solution temperature (LCST) at around 32 °C in water (25). Below the LCST, PNIPAM exists as a flexible conformation and is soluble in water. Above the LCST, the polymer becomes hydrophobic and the chains collapse. NIPAM has been polymerized for thermoresponsive delivery (24, 25), forming hydrogels for cell evaluation (26), and as smart coating for controlled release from gold nanocages (27). Cross-linked porous PNIPAM is a polymeric network capable of absorbing large amounts of water (28) while maintaining its distinct three-dimensional (3D) structure. The ability to absorb a vast quantity of water comes from the presence of the hydrophilic acrylamide group (29). Above the LCST, the swollen PNIPAM could contract in volume and squeeze the liquid out. In a previous study, thermoresponsive cross-linked PNIPAM with the in situ formation of organic nanoparticles was prepared by polymerizing NIPAM in the HIPEs followed by a freeze-drying process (30). The organic nanoparticles were released into water to form a stable aqueous nanoparticles dispersion via the contraction of porous PNIPAM in water when the aqueous phase was heated above the LCST. By using the HIPEs as templates, cross-linked PNIPAM was prepared with highly interconnected macropores and high pore volumes. The PNIPAM was able to absorb a large amount of water, thus making the polymeric network flexible and highly sensitive to water.

* Corresponding author. E-mail: zhanghf@liv.ac.uk. Tel: +44 151 7943545.
Received for review January 18, 2010 and accepted April 9, 2010

DOI: 10.1021/am100049r

Published on Web 04/27/2010

Table 1. Preparation Condition and Pore Characterization Data for Porous PNIPAM

sample	NIPAM (M)	MBAM (M)	pore size (μm) <LCST	pore size (μm) >LCST	pore volume (cm^3/g) <LCST	pore volume (cm^3/g) >LCST
PNIPAm-1	1	0.01	60.4,1.6	3.2	12.3	8.0
PNIPAm-2	1	0.02	60.5,0.8	3.9	9.9	4.7
PNIPAm-5	1	0.05	10.0	4.8	5.8	3.5

In this study, we wanted to investigate the use of highly porous PNIPAM to load and then release polymer colloids using temperature as the trigger. This is realized by swelling porous PNIPAM at room temperature to absorb aqueous colloidal suspensions and then releasing the loaded colloids via the contraction of PNIPAM above the LCST. Unlike the previous study where organic nanoparticles were formed simultaneously within the porous PNIPAM and released only from the formed nanoparticles (30), HIPE-templated porous PNIPAM is prepared and then used to load and release polymer colloids for multiple cycles. Because the process utilized the preformed polymer colloids, active ingredients such as drug molecules could be encapsulated into the colloids beforehand (31). This rendered the process very useful for the applications such as drug delivery. Polymeric microspheres (32), nanoporous colloids (33), microgels (34), and polymer vesicles (35) have been used as carriers for drug delivery. These delivery systems can be potentially employed in our proposed route. The utilization of porous PNIPAM as scaffold to accommodate the colloids which can then be released on demand using a temperature trigger may add an additional control over the release of the loaded components. Herein, we use polystyrene (PS) colloids as a model to show the multiple cycles of uploading and release in water by changing the surrounding temperature. Rhodamine B (a cationic dye) is attached to the PS colloid surface so that the loading and releasing behavior can be easily monitored by ultraviolet (UV) spectroscopy. A temperature-triggered loading and release of polymer colloids with porous PNIPAM acting like a pump is demonstrated.

EXPERIMENTAL SECTION

Chemical Regents. *N*-Isopropylacrylamide (97%, NIPAM), *N*,*N*′-methylenebisacrylamide (98%, MBAM), ammonium persulfate (98%, APS), Triton X-405 (70% in H_2O), *N*,*N*,*N*′,*N*′-tetramethylethylenediamine (99%, TMEDA), and rhodamine B (RhB) were purchased from Sigma-Aldrich and used as received; cyclohexane (CH) of analytical grade was from VWR. Methacrylic acid-stabilized PS colloids (10 wt %) with a zeta potential −45.2 mV were prepared according to the previously reported method (36) and then stained with RhB by placing a few crystals of the dye in the PS colloidal suspension and sonicated for 20 min. Excess dye was removed by filtering using a Gooch crucible and washed with copious amounts of water. Distilled water was used in all the experiments.

Synthesis of PNIPAM PolyHIPEs. The aqueous solution mixtures of NIPAM and MBAM with respective concentrations of 1.0 M and 0.0*x* M were prepared, designated PNIPAm-X (Table 1). The typical procedure for making PNIPAM with *x* % cross-linking comonomer was: aqueous NIPAM/MBAM solution (2.0 mL), Triton X-405 (0.3 mL), and APS (10% in H_2O, 0.1 mL) were added in turn while stirring at 600 rpm using a propeller stirrer, after which CH (6.0 mL) with TMEDA (30 μL) was slowly dropped into the aqueous phase. The phase volume ratio of oil to water in the emulsion was 3:1. The emulsion was kept stirring for 5 min and then placed in an oven at 60 °C for at least 12 h. The polymerized sample was allowed to cool down at room temperature, frozen rapidly in liquid nitrogen, and then freeze-dried at −10 °C in a freeze-dryer (VirTis Advantage, Biopharma) to produce a dry porous material. Porous PNIPAM was Soxhlet extracted with methanol and acetone (24 h each) at 120 and 140 °C, respectively, to remove the surfactant, APS, and unpolymerized monomers (13). The mass losses during extraction were 4.3% for PNIPAm-1, 4.0% for PNIPAm-2, and 3.9% for PNIPAm-5. There was no further mass loss observed when these samples were subjected to another cycle of extraction.

Procedure for Loading and Release of PS Colloids. Porous PNIPAM (0.05 g) was soaked in an aqueous suspension of RhB-stained PS colloids (10 mL, colloids concentration 3 ± 0.2 wt %) for 3 h. The swollen polymer was then filtered and surface water was wiped off. The colloids-loaded polymer was dried by freeze-drying. The mass loading was calculated by $(M_s - M_p)/M_p$ where M_s stands for the mass of the material after soaking and M_p stands for the mass of the polymer used.

PNIPAM loaded with the PS colloids was placed in a glass vial containing 10 mL water. The vial was placed into a fridge at 4 °C. 0.2 mL of the aqueous suspension was taken at different times for 2 h and stored for UV analysis. The removed medium volume was replaced by fresh water. After 2 h, the polymer was removed from the fridge and placed into a water bath at 45 °C. After 2 and 5 min in the water bath, two samples with each of them 0.2 mL were taken and stored for UV analysis. The 2 h release at 4 °C in the fridge and 5 min heating release in the 45 °C water bath with samples taken at different time intervals for analysis constituted one thermoresponsive release cycle. After that, the warmed samples were allowed to cool down for 1 h to room temperature. The samples were then placed back into the fridge for two more cycles of thermoresponsive release of PS colloids.

Both the upload and release procedures were repeated in order to test the repeating capability of uploading and releasing PS colloids. Instead of directly placing the cool samples in a fridge for the second cycle of thermoresponsive release, after the first cycle of release, the polymer was collected, dried, and weighed to get the mass of PS colloids left in the PNIPAM. The dry polymer with unreleased PS colloids was then immersed in the PS colloidal suspension for second upload, placed in a fridge for the release of PS colloids below the LCST, and then heated in the 45 °C water bath for the thermoresponsive release above the LCST. This constituted one cycle of upload and release process. Four cycles of upload and release of PS colloids were performed in this study.

The released percentage of loaded PS colloids was calculated for each cycle of loading and release. The mass of the polymer used was noted as Mp. The mass of the polymer after the first upload of the colloids was noted as M_∞. Each subsequent mass was measured as Mx. The percentage release was assessed by the equation [% release = $(M_x - M_p)/(M_\infty - M_p)$].

Characterization. The release of RhB-stained PS colloids was monitored using a 96-well UV plate reader (μQuant, Bio-Tek instruments Inc.) at wavelength 420 nm. All the PS colloidal suspensions were filtered using a 5 μm syringe filter before analysis. To assess the quantity of RhB-stained PS colloids in an aqueous suspension by UV analysis, we suspended known masses of the colloids in water and measured by UV to obtain a standard calibration curve of UV absorbance vs concentration of PS colloids. All the UV measurements in this study were in the linear region. The amount of PS colloids released into water was calculated based on the calibration curve. The porous structures and PS colloids were observed using a Hitachi S-4800 scanning electron microscope (SEM). The porous polymers were

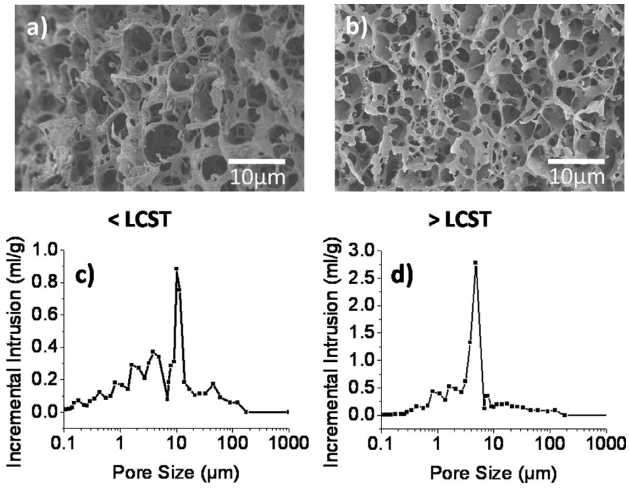

FIGURE 1. SEM images show the porous structures for 5% cross-linked PNIPAm-5 (a) below and (b) above the LCST. (c, d) Corresponding pore size distributions characterized by Hg intrusion porosimetry.

adhered to SEM studs using double-sided carbon tape and then coated with gold using a sputter-coater (EMITECH K550×) for 3 min at 40 μA before imaging. To image PS colloids with the SEM, 30 μL of the colloidal suspension (3 wt % or as released into water) was deposited and allowed to dry on an SEM stud and coated likewise. The pore volume and pore size distribution of porous PNIPAM were characterized by mercury intrusion porosimetry (Micromeritics Autopore IV 9500). The PS colloidal suspension was also analyzed by dynamic laser scattering (DLS, Viscotek model 802). Photographs of the polymer were taken using an Olympus C-5060 wide zoom digital camera.

RESULTS AND DISCUSSION

Emulsion-Templated PNIPAM. It was found that porous PNIPAM could absorb a large amount of the suspension and swell at room temperature. The swollen sample was then dried and weighed to calculate the mass loading of PS colloids. During this soaking process, the surfactant Triton X-405 and the unpolymerized monomers could also diffuse out of the porous PNIPAM. Moreover, the presence of nonthermoresponsive Triton X-405 in PNIPAM might reduce the temperature sensitivity and the volume change capacity. Therefore, the Soxhlet-extracted samples were used for all the loading and release studies.

Three levels of cross-linking (MBAM/NIPAM = 1, 2, and 5 mol %) were investigated. At the lower cross-linking ratio (1%), the PNIPAM was believed to be more flexible and more sensitive to temperature because the PNIPAM chains were less linked or "tied" by the cross-linker MBAM. The volume change was observed to be larger when the temperature was increased above the LCST by heating in a 45 °C water bath for 5 min. With the increase of cross-linking ratio, it was observed that the materials became more rigid and could be more easily handled with especially in the presence of water. At the cross-linking ratio 5%, a well-defined emulsion-templated porous structure was observed (Figure 1a). The average size of the open cells is around 10 μm. For the porous PNIPAM at the cross-linking ratios of 1 and 2%, the pore structures were rather similar, with larger pores being observed (see discussions for Figure 2 below).

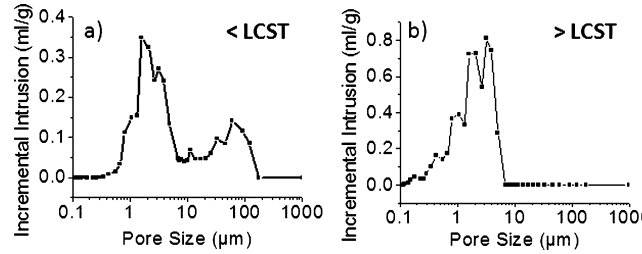

FIGURE 2. Pore size distributions of 1% cross-linked NIPAm-1 (a) below and (b) above the LCST measured by Hg intrusion porosimetry.

The volume change of porous PNIPAM below and above the LCST was reflected in the change of pore volume and pore size. This behavior was observed by SEM imaging and further characterized by mercury intrusion porosimetry. The porous PNIPAM was put into water and then stored for 15 min in a fridge at 4 °C. The swollen PNIPAM was filtered. After wiping off water on the material surface, the swollen sample was rapidly frozen in liquid nitrogen. It was then freeze-dried to represent the pore structure of PNIPAM below the LCST (Figure 1a). As comparison, the glass vial containing the swollen PNIPAM in water was heated in 45 °C for 5 min to make sure the temperature was above LCST. The water was taken out from PNIPAM while the vial was still in the water bath. It was important to freeze the warm PNIPAM with little surface water rapidly in liquid nitrogen in order to represent the pore structure of PNIPAM above the LCST. Figure 1b shows the SEM image of 5% cross-linked PNIPAM above the LCST. A decrease in pore size was observed, although it was not very obvious because of its highly interconnected pore structure. However, the decrease in pore size and pore volume could be clearly seen from the Hg intrusion data. As shown in Figure 1c, the pore size distribution was around 10 μm for 5% cross-linked PNIPAM below LCST. For the sample above LCST, the pore sizes were decreased with a distribution around 4.8 μm (Figure 1d). The pore volume was reduced from 5.8 cm^3/g (below LCST) to 3.5 cm^3/g (above LCST) due to the contraction of porous PNIPAM upon heating. At the lower cross-linking ratio (1 and 2%), porous PNIPAM was swollen in water to a larger degree. When the swollen material was heated in the water bath at 45 °C, the contraction ratio was also higher than that of PNIPAM with 5% cross-linking. A relatively large number of pores around 60 μm contributed to the larger pore volume for the PNIPAM with lower cross-linking (Table 1, Figure 2a).

Figure 2a shows the pore size distribution of 1% cross-linked porous PNIPAM. The double peak (60.4 and 1.6 μm) pore size distribution is observed. PNIPAm-2 exhibited a similar pore size distribution with double peaks around 60.5 and 0.8 μm. The large pores around 60 μm could be formed because of the templating of emulsion droplets and the coalescence of emulsion droplets during polymerization. The small pores around 1.0 μm could result from ice templating when the polyNIPAM was dried during a freeze-drying process. When a smaller amount of cross-linker MBAM was added, we observed that the polymerization was slower. It took a longer time for the emulsion structure to be locked by polymerization, thus leading to a partial destabilization

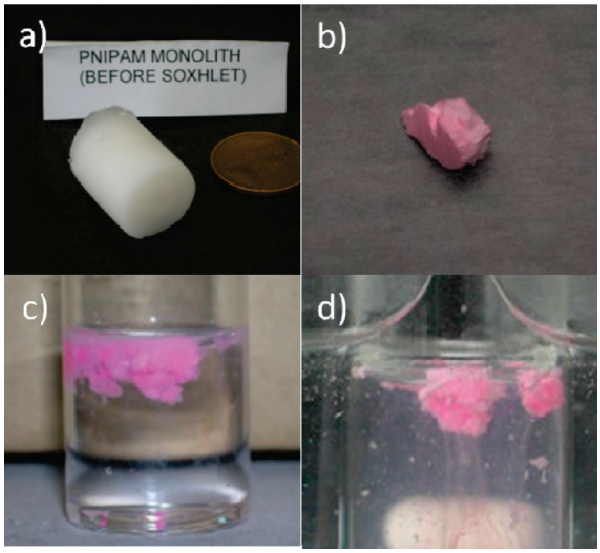

FIGURE 3. (a) As-prepared 1% cross-linked PNIPAM before Soxhlet extraction. (b) RhB-stained PS colloids-loaded PNIPAM. (c) PS colloids-loaded PNIPAM in water when placed in a fridge at 4 °C. (d) PNIPAM contracts and the colloids are released after heating in a 45 °C water bath.

of the emulsion and the coalescence of emulsion droplets. For Hg intrusion porosimetry, the pore sizes are measured and calculated when mercury is penetrated into the pores under different pressures. The pore size relates to the opening to the voids in the material rather than the diameter of the emulsion-templated pores. This is different from the pore sizes observed by SEM imaging which may indicate both void size and void opening size.

When the samples were heated in the 45 °C water bath, the pore size distribution around 60 μm disappeared for sample PNIPAm-1 (Figure 2b). This was thought to be due to the flexible polymer network at 1% cross-linking ratio and the collapse of large voids around 60 μm upon the contraction of PNIPAM in water above LCST. The pore volume was decreased from 12.3 cm^3/g to 8.0 cm^3/g accordingly (Table 1). A similar trend was observed for sample PNIPAm-2. For the same mass of porous PNIPAM, lower cross-linking ratio (1 and 2%) led to a larger volume contraction upon heating the sample above LCST. This was due to the small number of cross-linked points in the polymer, allowing a high flexibility within the chains of the PNIPAM. With regard to the swelling and contraction behavior in water, porous PNIPAM with 1 and 2% cross-linked ratios behaved in a similar way.

Uploading and Release of PS Colloids. The average diameter of the PS colloids was around 450 nm. The PS colloids precipitated overnight (>15 h) if the suspension stood still. However, the PS colloids could be readily resuspended by shaking. There was no aggregation or decreased stability observed after PS colloids were stained with RhB. The porous PNIPAM was white (Figure 3a). It should be noted that the PNIPAM monolith looked identical before and after extraction. After being soaked in the colloidal suspension and dried, the polymer turned red, indicating the loading of PS colloids (Figure 3b). Neither the aggregation nor the precipitation of RhB-stained PS colloids was observed in the water phase after the soaking process. To prove that all the RhB molecules were attached to the PS colloids rather than freely available in the aqueous phase, the RhB-stained colloidal suspension was centrifuged at 5000 rpm for 20 min. All the red PS colloids were precipitated. The supernatant water phase was colorless. This water phase was also analyzed by UV, showing no peak at 420 nm. This confirmed that it was the loading of PS colloids rather than free RhB that turned the PNIPAM red. Therefore, the UV absorption at 420 nm could reflect the concentration of PS colloids in water for the later release study.

The PS colloid-loaded PNIPAM was then placed in water for the temperature-triggered release of PS colloids. Scheme 1 illustrates how PS colloids were loaded into and then released from porous PNIPAM using temperature as a trigger. After loading PS colloids into PNIPAM (steps 1 and 2), the sample was swollen in water with no or few PS colloids being released (<LCST, stored in a fridge with temperature around 4 °C). Indeed, we did not observe the solution turning red for at least 2 h indicating very little release of RhB-stained PS colloids (Figure 3c, also see Figure 6). When the soaked sample in the vial was heated in a 45 °C water bath, it was clearly observed that the polymer started to contract and the pink cloud being diffused out of the sample (Figure 3d and step 3 in Scheme 1). As a result of RhB-stained PS colloids being released and suspended directly in water, the water phase turned red.

The average loadings of PS colloids based on the mass of PNIPAM from three measurements were obtained: 6.40% for PNIPAm-1, 2.65% for PNIPAm-2, and 0.83% for PNIPAm-5. It was found that the lower the cross-linking ratio, the higher the swelling capability and the higher loading of PS colloids could be achieved. After the loading of PS colloids,

Scheme 1. Schematic Representation for the Loading and Release of Colloids into and from Porous PNIPAM: (1) Soak Porous PNIPAm in a PS Colloidal Suspension below the LCST; (2) Filter and Dry to Obtain Colloids-Loaded PNIPAM below the LCST; (3) Place the Loaded PNIPAM in Water and Heat above the LCST to Release the Colloids

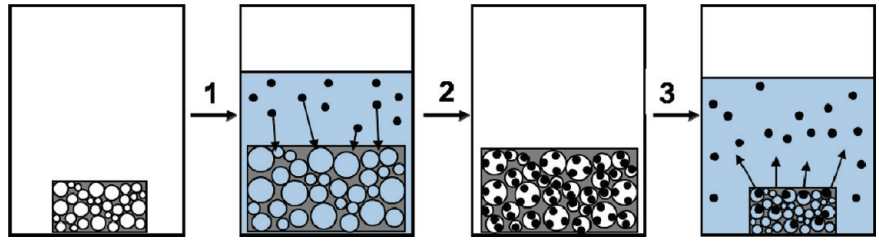

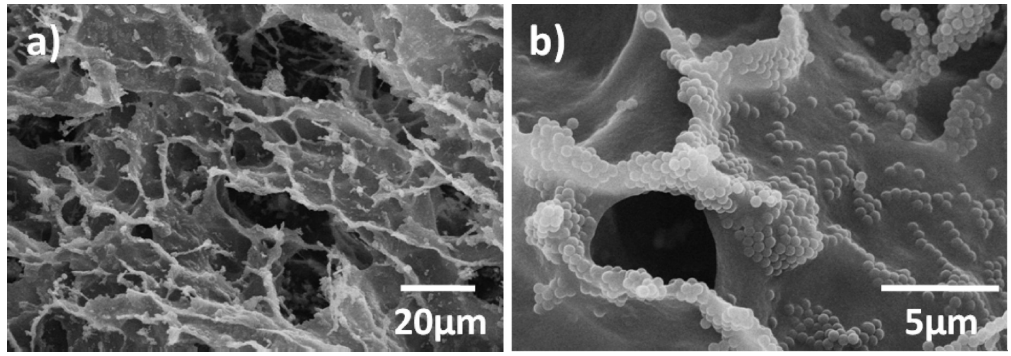

FIGURE 4. SEM images of PS-loaded PNIPAm-5 at (a) low and (b) high magnifications.

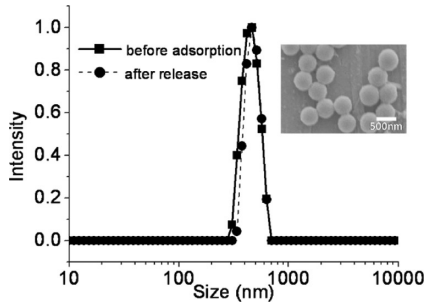

FIGURE 5. Particle size distributions of PS colloids before loading and after release as measured by DLS. The inset shows the SEM image of PS colloids after release.

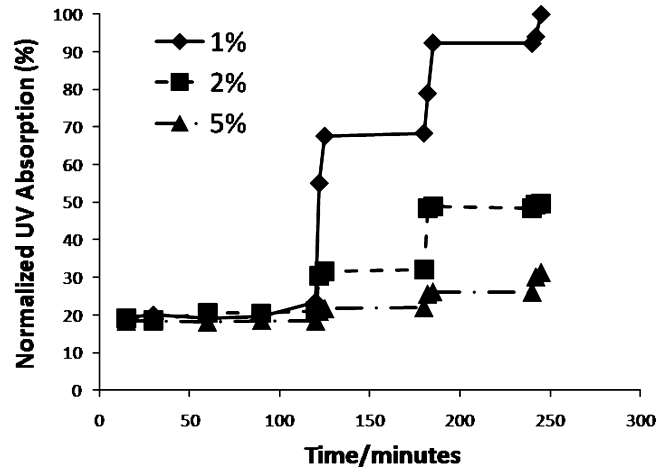

FIGURE 6. Three cycles of thermoresponsive release of PS colloids from porous PNIPAm at different cross-linking ratios (1, 2, and 5%).

the PNIPAM materials remained highly interconnected porous, as confirmed by the SEM (Figure 4a). The PS colloids were observed on the surface of the pores. However, the PS colloids were not seen to form a uniform layer on the surface. Instead, the PS colloids tended to aggregate on the edge of the pores (Figure 4b). This might be due to the possible stronger interaction between the PS colloids with negative surface charges and the amide groups on PNIPAM on the edge of the pores.

The RhB-stained PS colloids had an average diameter of 460 nm, as characterized by the DLS measurement and the SEM imaging (Figure 5 and the inset). When the PS colloids were released, a stable colloidal suspension like the original one was formed. No precipitate or aggregation of PS colloids was observed. The suspension of released PS colloids into water was characterized by DLS. As shown in Figure 5, the size distribution of PS colloids before loading and after release was very similar. This demonstrated that there was no aggregation of PS colloids occurring during the process of loading and release.

The release profiles of PS colloids below and above the LCST are shown in Figure 6 for porous PNIPAM with cross-linking ratios of 1, 2, and 5%. The same mass of PNIPAM samples was soaked in the same volume of PS colloidal suspensions with the same concentration. It was found that 1% cross-linked PNIPAM showed the highest PS colloids loading. The mass loading was the average data from three soaking experiments for PNIPAm-1, PNIPAm-2, and PNIPAm-5. Three cycles of release were performed for a temperature profile of from placing the samples in the fridge at 4 °C to heating the samples in a 45 °C water bath (see details in the experiment section). Sample PNIPAm-1 exhibited the highest release of PS colloids according to the UV absorption peaks. In order to compare the loading capacity and releasing behavior of PS colloids for PNIPAM at different cross-linking ratio, the UV absorption of released PS colloids was normalized against the maximum reading of PS colloids released from PNIPAm-1 after 3 heating cycles. The maximum absorption observed at 420 nm was denoted A_∞. All other absorptions from different samplings (A_t) were normalized by A_t/A_∞.

A step release profile was observed for each sample (Figure 6). When the PNIPAM loaded with PS colloids was placed in water at 4 °C, an 18% release of loaded PS colloids was observed by the first measurement at the fifteenth minute. The similar phenomena were observed for all the three samples. It was reasoned that the PS colloids on or close to the surface of the materials were suspended in water immediately. There was no further release of PS colloids from the PNIPAM for 2 h while the samples were placed in water at 4 °C. When these samples were heated in a 45 °C water bath, a burst release of PS colloids was seen and confirmed by the UV absorption. The samples were then stored in the fridge and two more heating cycles were performed. For sample PNIPAm-1, 50% of all the PS colloids loaded were released during the first heating cycle. Less PS colloids were released during the later heating cycles. It was quantified that 25 and 7% of all the PS colloids loaded were further released during the second and third heating cycles,

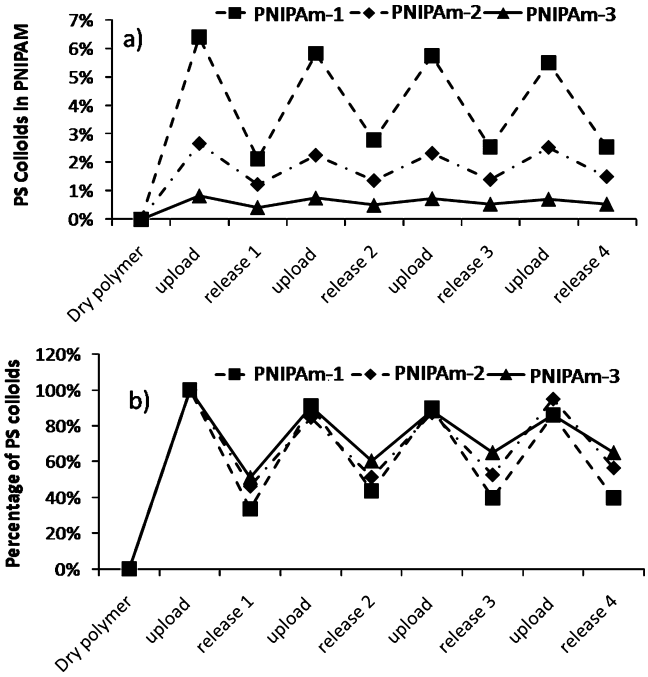

FIGURE 7. Four cycles of loading and release of PS colloids via porous PNIPAM. (a) Mass release of loaded PS colloids, shown as the mass percentage of loaded PS colloids based on the mass of PNIPAM. (b) Percentage release of loaded PS colloids.

respectively. Sample PNIPAm-1 had a higher loading capacity for PS colloids, which resulted from its more flexible polymer networks and ability to absorb a larger amount of PS colloidal suspension during the soaking process. Although samples PNIPAm-2 and PNIPAm-5 had lower loading capacity for PS colloids, the release profiles were similar during the three heating cycles (Figure 6), i.e., a higher percentage of PS colloids was released during the first heating cycles and less PS colloids were released in the later heating cycles. The percentage of release relative to the loading of PS colloids is discussed in the following section.

Repeated Loading and Release of PS Colloids. Considering the loading and release characteristic of the PS colloids, these porous PNIPAM might be referred as a pump to absorb and release the polymeric colloids in the presence of water simply by changing the surrounding temperature. However, to act like a pump, the porous materials should be able to perform many cycles of absorption and release. In this study, an initial effort was taken to demonstrate four cycles of loading and releasing PS colloids by porous PNIPAM.

In this study, the loading of PS colloids was presented as a percentage increase based on the mass of the polymer sample. Figure 7a shows the profiles of the mass loading and release in percentage based on the mass of PNIPAM. The loading of PS colloids was around 6.39 wt % for PNIPAm-1. Lower colloids loading were found for PNIPAM with higher cross-linking ratio (2.65 wt % for PNIPAm-2 and 0.85 wt % for PNIPAm-5). Around half or more loaded PS colloids were released during the heating cycle. The uptake of PS colloids by PNIPAM after one cycle of release was a bit lower but kept constant for the next three loading cycles. The performance profiles of repeated cycles of uploading and release were also presented in numerical figures in Table 2. It should be noted that not all the colloids loaded were released from the polymer during the heating cycle. There were three possible reasons: (1) when the polymer contracts, some small pores could "close over", thus trapping colloids from being released from the polymer; (2) the volume contraction ratio was limited and not all the colloids could be squeezed out; (3) the colloids could remain absorbed on the surface of the pores because the interaction between PS colloids and the PNIPAM networks.

The remaining PS colloids in PNIPAM could affect the further loading of PS colloids during the later soaking process. Our data showed that there was a slightly reduction in PS colloid loading for the 3 more cycles of soaking. Although not all the loaded PS colloids were released during the heating cycle, it seemed that most of the PS colloids from the second upload onward were released. For example, for PNIPAm_1 (Table 2), the first mass loading was 6.39% based on the mass of the polymer. The mass release of the loaded PS colloids was 4.26% (calculated by 6.39% − 2.13%). The mass increase was 3.69% (calculated by 5.82% − 2.13%) during the second upload while the mass release was 3.03% (5.82% − 2.79%). Similarly, for the third upload (2.95%) and fourth upload (2.95%), the mass releases were 3.2 and 2.95%, respectively. This was very important for the porous PNIPAM to act like a pump by uploading and release.

The data in Figure 7a were recalculated to show the percentage release of PS colloids in relation to the PS loading for each sample. The original mass of the dried polymer before loading was regarded as 0% with the first upload being 100%. The releasing profiles of four cycles of loading and release of PS colloids were shown in Figure 7b. By

Table 2. Performance Profiles of Repeated Cycles of Uploading and Release[a]

		1st cycle		2nd cycle		3rd cycle		4th cycle	
samples	release type	loading (%)	release (%)	loading (%)	release (%)	loading (%)	release (%)	loading (%)	release (%)
PNIPAm_1	mass	6.39	2.13	5.82	2.79	5.74	2.54	5.49	2.54
	percentage	100	33.33	91.03	43.59	89.74	39.74	85.90	39.51
PNIPAm_2	mass	2.65	1.22	2.24	1.36	2.31	1.39	2.52	1.50
	percentage	100	47.06	88.24	50.59	90.59	51.76	96.47	55.29
PNIPAm_3	mass	0.85	0.42	0.75	0.50	0.73	0.52	0.71	0.53
	percentage	100	55.91	89.25	60.22	90.33	62.37	95.70	65.59

[a] The mass release and percentage release of loaded colloids have the same meaning as in Figure 7. The numerical figures indicate the results after loading and release for four cycles of loading and release.

comparing the percentage loss of PS colloids during the releasing process, one could see a true picture of how the PNIPAM with different cross-linking ratios were able to release the loaded colloids. The sample PNIPAm-1 showed up to 65% release of the absorbed colloids for the first cycle and around 50% for later cycles (Table 2). The reloadings of the PS colloids were up to 90% of the original mass uptake. PNIPAm-2 gave a lower percentage of release with 53% release for the first cycle and around 40% for later cycle. The reabsorption of colloids reached approximately 90% of the initial uptake. Sample PNIPAm-5 had the lowest colloid release percentage with approximately 45% release of the loaded colloids for the first cycle and 30% release for later cycles (Table 2). Porous PNIPAM with a lower cross-linking density showed a higher swelling/contraction ratio and hence were able to release a larger amount of loaded colloids. For PNIPAM with a higher cross-linking ratio, the porous structure was rigid and a lower swelling/contraction ratio was observed. This led to a lower releasing capability for the loaded PS colloids. However, the reloading of PS colloids could reach 90% of the initial loading for all the three samples. This suggested that the repeated loading and release was effective even for the relatively highly cross-linked polymers.

The highest mass loading of PS colloids (6.4 wt %) was found during the first soaking process for sample PNIPAm-1. This loading was still quite low considering the high pore volume available in porous PNIPAM. However, this was very important for the release of PS colloids via the mechanism of swelling and contraction. As seen from the SEM image (Figure 4), the PS colloids were only covering the pore surface but not occupying or blocking the pores. This suggested that there was sufficient space for the PNIPAM to contract and the PS colloids could be released efficiently.

CONCLUSION

High internal phase oil-in-water emulsions were used as templates to prepare highly interconnected porous cross-linked PNIPAM. Porous PNIPAM swell in water when the temperature was below LCST and contracted when the water was heated above the LCST. This property was employed to load PS colloids at room temperature and then release the colloids when the solution was heated in a 45 °C water bath, with porous PNIPAM acting like a pump. Three release cycles and repeated loading and release of PS colloids were demonstrated. Importantly, for the multicycles of uploading and release, although not all the loaded PS colloids were released during the first heating cycle, most of the PS colloids from the second upload onward could be released. This method may be potentially useful for the controlled release of functional colloids or active-encapsulated colloids in applications such as drug delivery and smart coating.

Acknowledgment. We acknowledge the financial support from the EPSRC (EP/F016883/1). H.Z. is a RCUK academic fellow. We thank Mr. Nicolas Schaeffer for DLS measurements. The Centre for Materials Discovery is acknowledged for access to the state-of-the-art facilities.

REFERENCES AND NOTES

(1) Peppas, N. A.; Hilt, J. Z.; Khademhosseini, A.; Langer, R. *Adv. Mater.* **2006**, *18*, 1345–1360.
(2) Huebsch, N.; Mooney, D. J. *Nature* **2009**, *462*, 426–432.
(3) Cameron, N. R.; Sherrington, D. C.; Albiston, L.; Gregory, D. P. *Colloid Polym. Sci.* **1996**, *274*, 592–595.
(4) Zhang, H.; Cooper, A. I. *Soft Matter* **2005**, *1*, 107–113.
(5) Su, F.; Bray, C. L.; Tan, B.; Cooper, A. I. *Adv. Mater.* **2008**, *20*, 2663–2666.
(6) Christenson, E. M.; Soofi, W.; Holm, J. L.; Cameron, N. R.; Mikos, A. G. *Biomacromolecules* **2007**, *8*, 3806–3814.
(7) Kovacic, S.; Krajnc, P. *J. Polym Sci., A: Polym. Chem.* **2009**, *47*, 6726–6734.
(8) Zhao, C.; Danish, E.; Cameroon, N. R.; Kataky, R. *J. Mater. Chem.* **2007**, *17*, 2446–2453.
(9) Cameron, N. R. *Polymer* **2005**, *46*, 1439–1449.
(10) Williams, J. M.; Wrobleski, D. A. *Langmuir* **1988**, *4*, 656–662.
(11) Kulygin, O.; Silverstein, M. S. *Soft Matter* **2007**, *3*, 1525–1529.
(12) Zhang, H.; Cooper, A. I. *Chem. Mater.* **2002**, *14*, 4017–4020.
(13) Krajnc, P.; Stefanec, D.; Pulko, I. *Macromol. Rapid Commun.* **2005**, *26*, 1289–1293.
(14) Silverstein, M. S.; Tai, H.; Sergienko, A.; Lumelsky, Y.; Pavlovsky, S. *Polymer* **2005**, *46*, 6682–6694.
(15) Busby, W.; Cameron, N. R.; Jahoda, C. A. B. *Biomacromolecules* **2001**, *2*, 154–164.
(16) Lumelsky, Y.; Silverstein, M. S. *Macromolecules* **2009**, *42*, 1627–1633.
(17) Menner, A.; Verdejo, R.; Shaffer, M.; Bismarck, A. *Langmuir* **2007**, *23*, 2398–2403.
(18) Zhang, H.; Hardy, G. C.; Rosseinsky, M. J.; Cooper, A. I. *Adv. Mater.* **2003**, *15*, 78–81.
(19) Ikem, V. O.; Menner, A.; Bismarck, A. *Angew. Chem., Int. Ed.* **2008**, *47*, 8277–8279.
(20) Menner, A.; Ikem, V. O.; Salgueiro, M.; Shaffer, M. S. P.; Bismarck, A. *Chem. Commum.* **2007**, 4274–4276.
(21) Zhang, S.; Chen, J. *Chem. Commum.* **2009**, 2217–2219.
(22) Safinia, L.; Wilson, K.; Mantalaris, A.; Bismarck, A. *Macromol. Biosci.* **2007**, *7*, 315–327.
(23) Cummins, D.; Duxbury, C. J.; Quaedflieg, P. J. L. M.; Magusin, P. C. M. M.; Koning, C. E.; Heise, A. *Soft Matter* **2009**, *5*, 804–811.
(24) Gil, E. S.; Hudson, S. A. *Prog. Polym. Sci.* **2004**, *29*, 1173–1222.
(25) Schild, H. G. *Prog. Polym. Sci.* **1992**, *17*, 163–249.
(26) Klouda, L.; Hacker, M. C.; Kretlow, J. D.; Mikos, A. G. *Biomaterials* **2009**, *30*, 4558–4566.
(27) Yavuz, M. S.; Cheng, Y.; Chen, J.; Cobley, C. M.; Zhang, Q.; Rycenga, M.; Xie, J.; Kim, C.; Song, K. H.; Schartz, A. G.; Wang, L. V.; Xia, Y. *Nat. Mater.* **2009**, *8*, 935–939.
(28) Mano, J. F. *Adv. Eng. Mater.* **2008**, *10*, 515–527.
(29) Peppas, N. A.; Khare, A. R. *Adv. Drug Delivery Rev.* **1993**, *11*, 1–35.
(30) Zhang, H.; Cooper, A. I. *Adv. Mater.* **2007**, *19*, 2439–2444.
(31) Freitas, S.; Merkle, H. P.; Gander, B. *J. Controlled Release* **2005**, *102*, 313–332.
(32) Freiberg, S.; Zhu, X. X. *Int. J. Pharm.* **2004**, *282*, 1–18.
(33) Wang, Y.; Price, A. D.; Caruso, F. *J. Mater. Chem.* **2009**, *19*, 6451–6464.
(34) Saunders, B. R.; Laajam, N.; Daly, E.; Teow, S.; Hu, X.; Stepto, R. *Adv. Colloid Interface Sci.* **2009**, *147−148*, 251–262.
(35) Li, M. H.; Keller, P. *Soft Matter* **2009**, *5*, 927–937.
(36) Zhang, H.; Lee, J. Y.; Ahmed, A.; Hussain, I.; Cooper, A. I. *Angew. Chem., Int. Ed.* **2008**, *47*, 4573–4576.

AM100049R